Cement and Concrete Research 38 (2008) 1394–1400

Contents lists available at ScienceDirect

Cement and Concrete Research

journal homepage: http://ees.elsevier.com/CEMCON/default.asp

Physical modeling of the electrical double layer effects on multispecies ions transport in cement-based materials

H. Friedmann, O. Amiri *, A. Aït-Mokhtar

Université de La Rochelle, LEPTIAB, Av. M. Crépeau 17042 La Rochelle Cedex 1, France

ARTICLE INFO

Article history:
Received 7 May 2007
Accepted 10 June 2008

Keywords:
Diffusion
Electrochemical properties
Transport properties
Cement
Fluxes

ABSTRACT

The transport of ions through cement-based materials is described at a microscopic scale with a pore modeled by two infinitely large flat plates. The theory of the electrical double layer (EDL) shows that (i) the overlapping between the diffuse layers occurring in the pore is more important as the pore diameter will be small (low than the Debye length) and the pore walls will be strongly charged, (ii) the fluxes of coions and counterions will be respectively increased and attenuated in such pores. The gel pores of cement based materials have similar characteristics. As the capillary pores of the cement based materials with low porosity are connected between them by the pores gel, the transport of ions at a macroscopic scale could be greatly influenced by the overlapping effect of the diffuse layers.

1. Introduction

Many concrete structures are affected by corrosion of reinforced bars due to the chlorides. A better understanding of ionic transport phenomena, specifically the chlorides through concrete would, improve the service life of these structures. Ionic transport mechanisms through cement-based materials are generally described by the set of the Nernst–Planck equation, conservation equations combined sometimes with electroneutrality condition [1–4]. Some of the characteristics of the material are introduced in the modeling:

(i) the chemical reactivity between the porous materials and the ions involved in the transport and;
(ii) the morphology of the porous network.

The first point is considered in literature by adsorption isotherms and the second point is expressed in a global parameter, called the formation factor [3,4]. The mono-species models which consider only on chloride have shown difficulties to fit experimental data [5]. More recently some researchers have developed multi-species approaches which are more rigorous but more complex [3,4]. There are very few works on the experimental validation of these models on the cement-based materials [6].

Others physicochemical phenomena involved in cement based materials could be introduced in the different models but they are generally regarded as secondary: this is often the case of the electrical double layer (EDL) which occurs at the interface between pore walls and pore solution [7]. The EDL phenomena are of a particular interest if we consider the importance of the interface between the electrolyte filling the pores and the solid matrix of the porous medium. For example, in the field of nanofiltration membranes, the EDL takes a significant part in the modeling of transport phenomena [7]. The choice to introduce the EDL in modeling transport phenomena through a porous medium depends on different factors like the size of the pore and of the charge carried out by the interface. Some researchers have been interested with this subject [9–14] in the field of cement-based materials but works dealing with the coupling between EDL and transport phenomena remain rather marginal: we can note the works of Amiri et al. [15,16], which studied the EDL effect by a fundamental approach.

The aim of this paper is to model, at a microscopic scale and in a multispecies approach, the coupling between transport phenomena and the EDL in order to quantify their effects on the ionic transport through cementitious materials. For this purpose, a physical modelling is carried out to investigate transport processes in the pore solution.

2. Description of the electrical double layer phenomenon: an overview

The EDL phenomena is described in many textbooks [17–23]. Historically, Quincke (1861) and Helmholtz (1879) were the first who have proposed a description of the phenomena involved at the solid–liquid interface by performing similarities with electrical circuits. In their approach, the interface is modeled by a plane condenser (Fig. 1.a) made up by ions present in the solid phase and ions of opposite charge in the solution, separated by a distance d corresponding to the water molecule diameter.

* Corresponding author. Tel.: +33 546 45 86 24; fax: +33 546 45 82 41.
E-mail address: oamiri@univ-lr.fr (O. Amiri).

0008-8846/$ – see front matter © 2008 Elsevier Ltd. All rights reserved.
doi:10.1016/j.cemconres.2008.06.003

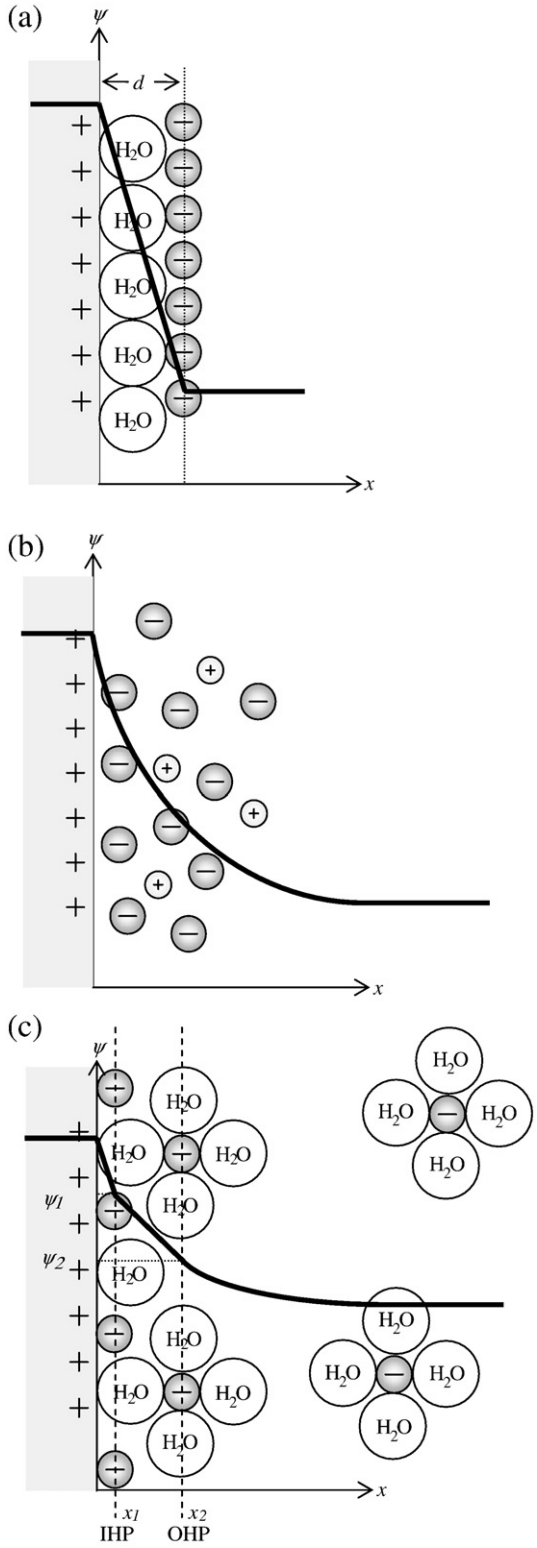

Fig. 1. Schematic modeling of the EDL: solid-electrolyte interface and distribution of the electrical potential ψ according to different authors: (a) Helmholtz model, (b) Gouy–Chapman model, (c) Grahame model.

The exceeding electrical charge q_s, carried by the solid phase, is neutralised by a monolayer of ions of opposite charge q, "the counterions", on the electrolyte side such as $q_s = -q$. The drop of the electric potential is linear. The interface is similar to a condenser with a capacity C_H:

$$C_H = \frac{\varepsilon_H}{d} \tag{1}$$

where ε_H is the dielectric permittivity of the interfacial space.

The Helmholtz theory fails to correctly explain some experimental results dealing with the variation of the capacity in function of the difference of potential between solid phase and liquid phase [18,20].

Gouy (1910) and Chapman (1913) improved the Helmholtz model by taking into account the thermal motion of ions, which tends to disperse these ions. Therefore, in comparison with the Helmholtz's model, the Gouy–Chapman's model includes an electrically charged volume of liquid in the vicinity of the interface. In this volume, called "diffuse layer", counterions are more concentrated than "the coions". Fig. 1.b shows a diffuse layer negatively charged consisted of anions attracted by the solid phase, while cations, less concentrated, are pushed back to the bulk of the pore solution. The potential profile is no more linear as in the Helmholtz model and must be determined according to the Poisson–Boltzmann equation (see Section 2.1).

However, the Gouy–Chapman model is not satisfactory: ions are regarded as punctual charges being able to approach the solid phase until the distance between them and the interface is zero. The capacities calculated with this theory are not in agreement with experimental results [18,20]. In 1924, Stern proposes a combination of the previous approaches in which the charged domain is structured in two parts, a diffuse layer and a compact layer: this model is called the electrical double layer. The compact layer is made of solvated ions, adsorbed at the surface.

Grahame (1952) improves the Stern model by considering the possibility of a chemical adsorption called "specific adsorption". This kind of adsorption is chemical and depends on the nature of ions and on the solid surface. In this type of interaction, the charges of the adsorbed ions could be of an opposite sign to the EDL one's. The compact layer is divided into two parts: the centre of specifically adsorbed ions defines the inner Helmholtz plane (IHP) $x = x_1$, while the centre of non-specifically adsorbed ions defines the outer Helmholtz plane (OHP) $x = x_2$. ψ_2 is the electrical potential in the outer Helmholtz plane (Fig. 1-c) corresponding to the closest approach plane.

To describe transport phenomena trough cement-based materials, we have adopted in this work the Stern model (which is a particular case of Grahame model). In the vicinity of the interface, ions in the pore solution can be classified into two types, separated by the closest approach plane (Fig. 2):

- ions which are considered adsorbed, i.e. bound to the solid phase; they are quantified by an adsorption isotherm, without distinction between specifically and non-specifically adsorbed ions;
- ions present in the diffuse layer, i.e. free which take part in transport phenomena.

Equations relating to the EDL phenomena are presented with the coordinates system defined in Fig. 2: *Ox* is an axis perpendicular to a surface element, which separates the solid phase from the pore solution. The axis origin $x = 0$ corresponds to the closest approach plane. In this plane, the potential is called OHP potential and noted ψ_0. So, diffuse layer extends from the OHP to the bulk solution.

We can also define the shear plane which is the plane separating the thin layer of liquid bound to the solid surface from the rest of the liquid. The potential at this plane is called the zeta potential, ζ, and can be measured by a zeta meter [9,14]. The shear plane and the OHP potential being very close, ζ and ψ_0 are assumed to be similar in this work [8,24]. According to Londiche [25], the usual value range of the zeta potential measured with respect to the bulk electrical potential is from −100 mV to 100 mV.

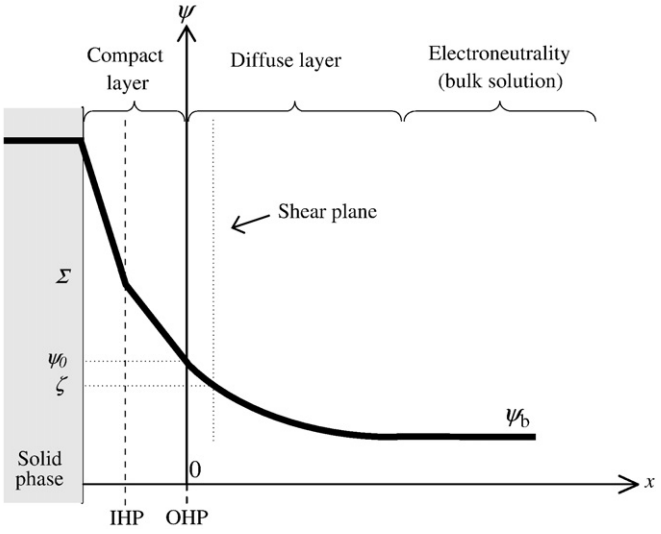

Fig. 2. Schematic view of the EDL model used.

2.1. Fundamental equations

To describe the EDL phenomena at a microscopic scale, we consider the following assumptions:

- the pores are saturated;
- the convection of the pore solution is neglected;
- the pore solution is composed of monovalent ions;
- the solid phase does not conduct current;
- the dielectric permittivity is the same all over the pore solution as well in the diffuse layer as in the bulk solution;
- the temperature is uniform and constant.

In this paper, all the quantities referred to the bulk solution will be subscripted with the letter *b*. All the potential in the diffuse layer will be defined with respect to the bulk electric potential on the *Ox* axis (Fig. 2). Also, if ψ is an electric potential of the diffuse layer, $\delta\psi$ is the electrical potential measured with respect to the electrical potential in the bulk solution $\delta\psi = \psi - \psi_b$.

In this case, the electric potential ψ distribution along the *Ox* axis is the solution of the Poisson–Boltzmann equation (PB) [22]:

$$\frac{\partial^2 \delta\psi_+}{\partial x_+^2} = \sinh \delta\psi_+ \tag{2}$$

which is a combination of the Poisson equation:

$$\Delta\psi = -\frac{\rho}{\varepsilon} \tag{3}$$

and Boltzmann distribution (Eq. (5)).

Assuming that there is no ionic flux along the *Ox* axis, the Nernst–Planck equation is written:

$$-D_k \frac{\partial c_k}{\partial x} - \frac{F}{RT} z_k D_k c_k \frac{\partial \psi}{\partial x} = 0 \tag{4}$$

D_k, z_k and c_k are, respectively, the diffusion coefficient, the valence and the concentration of species *k*, ε is the dielectric permittivity of the solution, ψ is the electrical potential at the considered point, *R* is the gas constant, *T* the thermodynamic temperature, *F* the Faraday constant. The volumetric charge density ρ is defined by the Boltzmann distribution:

$$\rho = F\sum_k z_k c_k = -2Fc_b \sinh \delta\psi_+ \tag{5}$$

x_+ and $\delta\psi_+$ are respectively the dimensionless length and the electrical potential defined as:

$$\delta\psi_+ = \frac{F}{RT}\delta\psi \tag{6}$$

$$x_+ = \kappa x \tag{7}$$

κ being the Debye constant [22]:

$$\kappa = \sqrt{\frac{2F^2 c_b}{RT\varepsilon}} \tag{8}$$

and $1/\kappa$ represents length, which characterises the extension of the diffuse layer.

c_b is the concentration of the cations or anions (indifferently) in the bulk solution because (i) the Poisson equation can be replaced with a good approximation by the electroneutrality condition [19] and (ii) we are considering an electrolyte composed of monovalent ions.

The solution of the PB (Eq. (2)) equation is [15]:

$$\delta\psi_+ = 2\ln\left(\frac{1+\tanh\frac{\delta\psi_{+0}}{4}\exp(-x_+)}{1-\tanh\frac{\delta\psi_{+0}}{4}\exp(-x_+)}\right) \tag{9}$$

Then, the concentration distribution in the diffuse layer is given by the solution of Eq. (4):

$$c_k = c_{kb}\exp(-z_k\delta\psi_+) \tag{10}$$

and with Eq. (9), we have:

$$c_k = c_{kb}\left(\frac{1+\tanh\frac{\delta\psi_{+0}}{4}\exp(-x_+)}{1-\tanh\frac{\delta\psi_{+0}}{4}\exp(-x_+)}\right)^{-2z_k} \tag{11}$$

The equivalent surface charge density *q* for the EDL can be deduced from the volumetric charge density:

$$q = \int_0^\infty \rho(x)dx \tag{14}$$

which can be written [20]:

$$q = -\sqrt{8RT\varepsilon c_b}\sinh\frac{\delta\psi_{+0}}{2} \tag{17}$$

Principal results can be summarized as follows. Eq. (9) shows that the electric potential varies along the diffuse layer from the value of the OHP potential to the value of electric potential of the bulk solution, as represented on the Fig. 2. The concentration of counterions in the diffuse layer is thus much larger than the coions concentration (Eq. (11) and Fig. 3). Consequently, the volumetric charge density varies from a negative or a positive value to gradually reach a zero value, corresponding to the electroneutrality condition in the bulk solution i.e. the equality of concentrations between coions and counterions. The domain of validity of electroneutrality in the vicinity of the interface is function of the Debye length, i.e. of the concentration of the bulk solution (Eq. (8)): the more the ionic concentration of the bulk solution is weak the more the Debye's length is large.

The evolution of the electric potential and the sign of the volumetric charge density in the diffuse layer depend on the sign of $\delta\psi_0$ (Eq. (9)):

if $\delta\psi_0 < 0$, $\delta\psi$ increases, the counterions are cations and the diffuse layer is of positive charge;

if $\delta\psi_0 > 0$, $\delta\psi$ decreases, the counterions are anions and the diffuse layer is of negative charge.

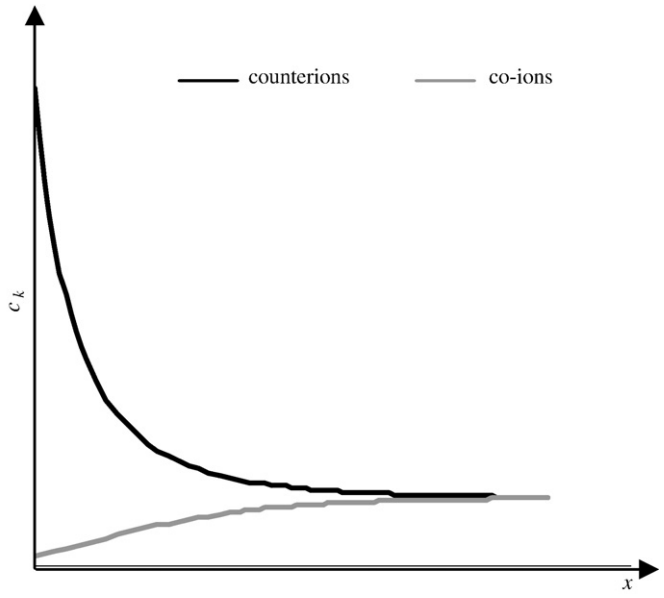

Fig. 3. Distribution of the ions in the diffuse layer.

2.2. Case of a pore

In this section, we are considering that a pore of a porous medium can be schematically represented by two parallel flat plates A and B at distance L and separated by the electrolyte (Fig. 4). Ox is an axis perpendicular to these planes and r is located at $L/2$. This assumption is considered as a first approach, in order to simplify calculations. In fact, the network of cement based materials is more complex.

In this case, two diffuse layers are face to face. The distribution of the electric potential is solved using the PB equation (Eq. (2)) and taking into account the symmetry condition:

$$\left|\frac{\partial \delta\psi_+}{\partial x}\right|_{x=r} = 0 \tag{12}$$

A first integration of the PB equation yields:

$$\frac{\partial \delta\psi_+}{\partial x_+} = -\sqrt{2(\cosh \delta\psi_+ - \cosh \delta\psi_{+r})} \tag{13}$$

where $\delta\psi_{+r}$ is the value of $\delta\psi_+$ at $x=r$.

The Eq. (13) is then solved numerically according to the method developed by Dubois et al. [26].

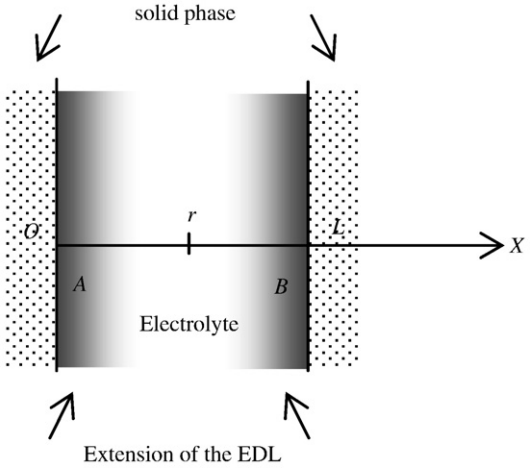

Fig. 4. Schematic representation of a pore cross-section.

Results are given for a solution close to that of the pore solution in cement-based materials, i.e. composed of monovalent ions (Na^+, K^+ and OH^-) with a cation (or anion) concentration of 0.1 mol l^{-1} according to Schmidt and Rostasy [27]. In this case and for a temperature of 25 °C, the Debye length is 0.97 nm (from Eq. (8)). We can note that the cement based materials may have ion concentration as high as 0.7 molar. In this condition, the Debye length will be shorter and the EDL effect will be presumably small. However, if the materials are immersed (water, seawater), leaching phenomena will occur, which leads to impoverishment of the ionic solution. Then, the concentration of the pore solution will slow-down, and could reach a weak value, that makes the EDL effect not negligible.

The calculation is carried out for a pore size close to the Debye length, 2 nm, in order to show the overlapping phenomenon. This diameter represents a mean value of C–S–H pores. A discussion about the presence of this pore dimension in cement-based materials will be developed in Section 4.

Concerning the OHP potential in cement-based materials, it is difficult to find values in the few works dealing with this subject [9,13,14]. Because of lack of suitable values to the cement-based materials, a large enough value of 50 mV was chosen in order to emphasise the overlapping effect.

The distribution of the electric potential across the pore section is represented in Fig. 5. The electric potential values are then included in Eq. (10) in order to determine the concentration profiles of coions and counterions (Fig. 6).

Fig. 6 shows the overlapping effect of the diffuse layers. Whatever the value of the coordinate x, one notes an important variation between the concentration of counterions and coions: there is no electroneutrality and the pore is entirely charged electrically. But if the pore diameter L is large compared to the Debye length $1/\kappa$, there is no overlapping; in this case, the EDL modifies the different ionic concentration at the vicinity of the plates but not at the center of the pore, where the electroneutrality is verified: the diffuse layers are distinct one from the other.

2.3. Importance of overlapping in function of the pore diameter

For a given constant Debye length, the importance of the overlapping depends on the pore diameter L. It can be quantified by the expression of the volumetric charge density at the pore center $x=r$:

$$\rho(r) = F(z_{co}c_{co}(r) + z_{ct}c_{ct}(r)) \tag{14}$$

where $c_{co}(r)$, $c_{ct}(r)$, z_{co} and z_{ct} are the concentrations of co-ions and counterions and their valence in the pore center, respectively. The

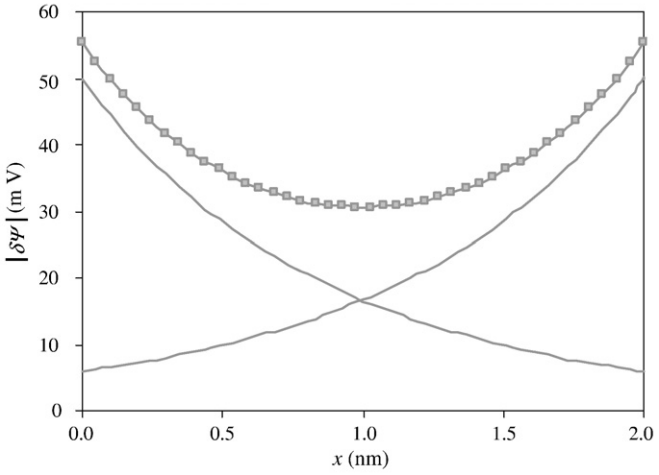

Fig. 5. Electric potential profile $\delta\psi$ for $L=2$ nm. Solid line with square data points, numerical resolution with overlapping; grey solid line, solution without overlapping.

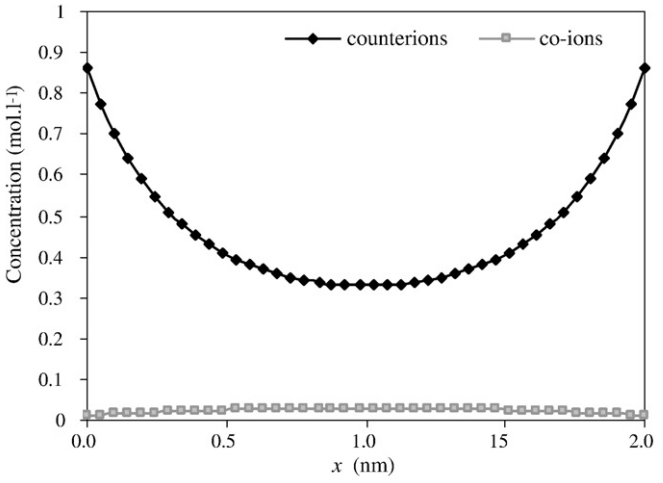

Fig. 6. Concentration profiles of coions and counterions for L=2 nm.

evolution of the absolute value of the volumetric charge density ρ in function of the pore diameter L is presented in Fig. 7 for three values of the OHP potential $\delta\psi_0$ and with a Debye length of 0.97 nm as in the previous section.

Fig. 7 shows that the overlapping starts to appear below a diameter of pore, which is independent of the OHP potential value. Indeed, the length Debye which determines the occurring of the overlapping for a given diameter, is a function of the bulk solution concentration c_b and not of the OHP potential (Eq. (10)). For lower diameters, the overlapping is more important as the OHP potential is larger since for the same length of Debye (thus the same value of c_b), more $\delta\psi_0$ is larger, more the diffuse layer is electrically charged. The overlapping phenomenon will be thus more important as the pore diameter will be small and pores walls will be strongly charged.

3. Transport equations at microscopic scale

We showed previously that the EDL modifies the concentration of an ionic species k across a pore section. Consequently, the ion fluxes of the species present in the pore solution are also affected by the EDL. As in the previous section, we are considering the transport of ions between the two parallel plates A and B as described on Fig. 4. The following assumption is added to those mentioned in the Section 2.1: the concentration c_{kb} of an ionic species outside of the EDL is considered uniform over a pore cross-section. Therefore, the gradient of concentration and consequently the electrical field in the bulk solution are perpendicular to a cross-section.

3.1. Mean value of ionic concentration and flux over a cross section

First, a homogenization technique is applied to the concentration over a cross-section. Heterogeneities are thus averaged to give only one mean value of the concentration and flux. The mean concentration $\bar{c}_k$ is defined by:

$$\bar{c}_k = \frac{1}{L}\int_0^L c_k dx \tag{15}$$

and with Eq. (10) we have:

$$\bar{c}_k = \overline{c_{kb}\exp(-z_k\psi_+)} = \overline{\exp(-z_k\psi_+)}c_{kb} \tag{16}$$

By taking into account the assumptions presented in Section 2.1, the ion flux of a species k within a pore is written by the Nernst–Planck [18] equation as follows:

$$\vec{j}_k = -D_k\ \overrightarrow{grad}c_k - z_k D_k c_k\ \overrightarrow{grad}\psi_+ \tag{17}$$

To include EDL phenomena in the ionic transport mechanisms, the Eq. (10) is introduced in the above Eq. (17):

$$\vec{j}_k = -D_k\ \overrightarrow{grad}\{c_{kb}\exp(-z_k\delta\psi_+)\} - z_k D_k c_{kb}\exp(-z_k\delta\psi_+)\ \overrightarrow{grad}\psi_+ \tag{18}$$

one obtains finally:

$$\vec{j}_k = \exp(-z_k\delta\psi_+)\ \vec{j}_{kb} \tag{19}$$

with:

$$\vec{j}_{kb} = -D_k\ \overrightarrow{grad}c_{kb} - z_k D_k c_{kb}\ \overrightarrow{grad}\psi_{+b} \tag{20}$$

where $\vec{j}_{kb}$ is the ion flux of the species k in the bulk solution. So, it can be noticed that the flux is not the same all over the cross-section. Eq. (19) thus shows that the flux of counterions increases in the EDL with regard to the bulk while that of coions decreases since $z_{ct}\delta\psi_+<0$ and $z_{co}\delta\psi_+>0$.

Heterogeneities of the flux over a pore cross-section are also averaged to give only one mean value $\bar{\vec{j}}_k$:

$$\bar{\vec{j}}_k = \frac{1}{L}\int_0^L \vec{j}_k dx \tag{21}$$

Thus, the mean flux in a cross-section is:

$$\bar{\vec{j}}_k = \overline{\exp(-z_k\psi_+)\vec{j}_{kb}} = \overline{\exp(-z_k\psi_+)}\,\vec{j}_{kb} \tag{22}$$

For example, in the case of the concentration distribution presented in Section 2.2 (Fig. 6), the average concentration of coions and counterions $\bar{c}_{co}$ and $\bar{c}_{ct}$ calculated by a trapezoidal method are $\bar{c}_{co}$=0.0234 mol l^{-1} and $\bar{c}_{ct}$=0.4626 mol l^{-1}, i.e. $\bar{c}_{ct}$=19, $8\bar{c}_{co}$.

3.2. Analytical calculation of the mean value of concentration and flux

In the case of an overlapping of the diffuse layers (Fig. 6), we see in Section 2.2 that the calculation of the electric potential $\delta\psi$ and concentration profile c_k in a pore cross-section requires a numerical method. Dufrêche et al. [28] showed that it is possible to correctly express the average concentration of the ions by using an approximation of Pade between two areas of extreme concentrations c_b (weak

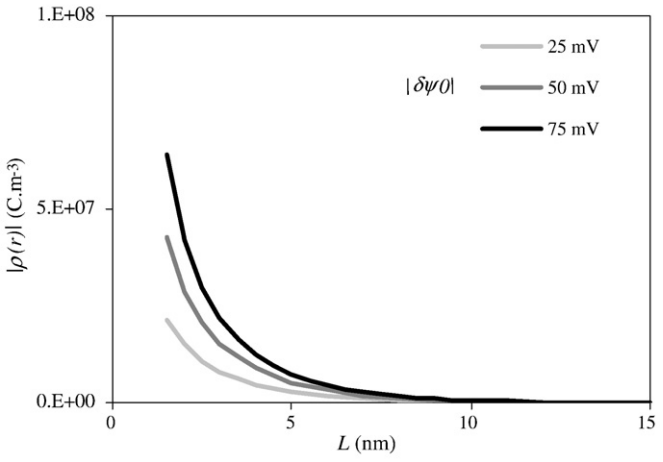

Fig. 7. Evolution of the absolute value of the volumetric charge density ρ in the pore center in function of the pore diameter L.

and strong concentration). Thus, according to their approximation, the mean concentration of co-ions is:

$$\frac{\overline{c}_{co}}{c_b} = \frac{Ad_+^2}{1 + ABd_+ + Ad_+^2} \tag{23}$$

with

$$A = \frac{1}{8\pi^2}\left(1 + \frac{3}{F_0}\right) \quad \text{and} \quad B = 4\left(\exp\left(\frac{\delta\psi_{+0}}{2Z}\right) - 1\right) \quad \text{and} \quad F_0 = \frac{qFd}{4ZRT\varepsilon} >> 1 \tag{24}$$

The mean volumetric charge density over a cross-section is written:

$$\overline{\rho} = F(z_{co}\,\overline{c}_{co} + z_{ct}\,\overline{c}_{ct}) = \frac{2q}{d} \tag{25}$$

with q, the surface density of charge.

The concentration of counterions is thus:

$$\frac{\overline{c}_{ct}}{c_b} = \frac{Ad_+^2}{1 + ABd_+ + Ad_+^2} - \frac{2q}{Fdc_b} \tag{26}$$

One deduces that:

$$\overline{\exp(-z_{co}\psi_+)} = \frac{Ad_+^2}{1 + ABd_+ + Ad_+^2} \tag{27}$$

while:

$$\overline{\exp(-z_{ct}\psi_+)} = \frac{Ad_+^2}{1 + ABd_+ + Ad_+^2} - \frac{2q}{Fdc_b} \tag{28}$$

The mean flux relation (22) can thus be written for the coions and counterions respectively as:

$$\overline{\vec{j}}_{co} = K_{co}\,\vec{j}_b \tag{29}$$

$$\overline{\vec{j}}_{ct} = K_{ct}\,\vec{j}_b \tag{30}$$

where K_{co} and K_{ct} are EDL effect on the ionic fluxes in the bulk solution and defined for coions and counterions, respectively by:

$$K_{co} = \overline{\exp(-z_{co}\psi_+)} = \frac{Ad_+^2}{1 + ABd_+ + Ad_+^2} \tag{31}$$

$$K_{ct} = \overline{\exp(-z_{ct}\psi_+)} = \frac{Ad_+^2}{1 + ABd_+ + Ad_+^2} - \frac{2q}{Fdc_b} \tag{32}$$

The concentrations of coions and counterions are written as:

$$\overline{c}_{co} = K_{co}c_b \tag{33}$$

$$\overline{c}_{ct} = K_{ct}c_b \tag{34}$$

The values of K_{co} and K_{ct} obtained respectively with Eqs. (31) and (32) are presented in Table 1 for one example of diameter (L=2 nm).

Table 1
Values of K_{co} and K_{ct}, analytically and numerically calculated

Pore diameter L (nm)		2
$\delta\psi_0$ (mV)		50
c_b (mol l^{-1})		0.1
K_{co}	(Eq. (31))	0.20
	numerical resolution (Eq. (13)) of $\delta\psi_+$	0.23
K_{ct}	(Eq. (32))	4.60
	numerical resolution (Eq. (13))of $\delta\psi_+$	4.63

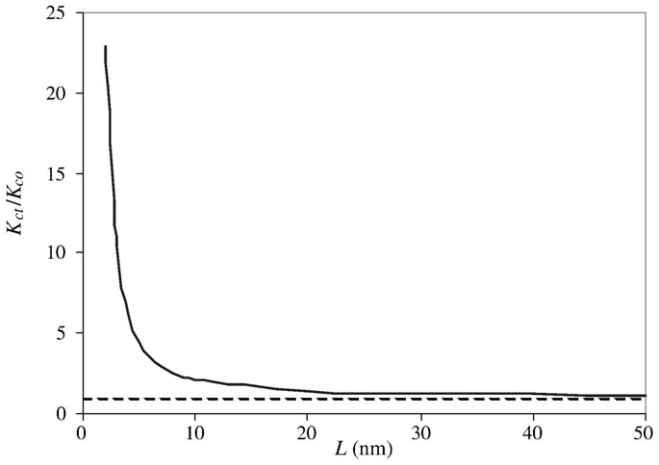

Fig. 8. Ratio K_{ct}/K_{co} versus the pore diameter with a bulk concentration of 0.1 mol l^{-1} and a OHP potential of 50 mV.

For comparison, we also presented the values of K_{co} and K_{ct} obtained from Eqs. (31) and (32) but with the values of $\delta\psi_+$ calculated numerically in Section 2.2.

Analytical results using Pade approximation (Eqs. (31) and (32)) give similar results to those obtained numerically. Thus, we can note that Pade approximation is useful and the numerical calculation, which is time consuming, can be avoided.

On Table 1, we can note that K_{ct}>1 and K_{co}<1. This means that the flux of coions and that of counterions will be respectively attenuated and amplified compared to the flux in the bulk solution; this phenomenon is depending on the overlapping of the diffuse layers. Figs. 8 and 9 show respectively the ratio between the coefficient K_{ct} and K_{co} (calculated with the Pade approximation) versus the diameter with a constant OHP potential and versus the OHP potential with a constant pore diameter in the same condition of concentration as previously described (see Section 2.2).

It can be seen on Fig. 8 that below a pore size diameter of 10 nm, the ratio K_{ct}/K_{co} is higher than 2: the mean concentration and flux of counterions are at least twice higher than those of coions. For a constant pore diameter of 2 nm, Fig. 9 shows that the same ratio is obtained for an OHP potential higher than 8 mV.

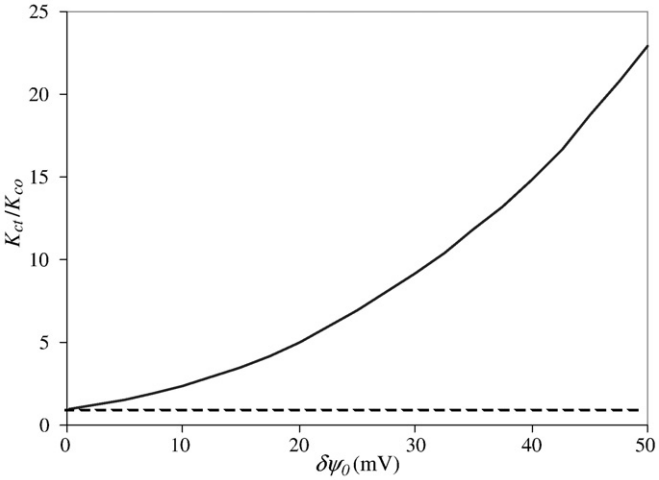

Fig. 9. Ratio K_{ct}/K_{co} versus the OHP potential with a bulk concentration of 0.1 mol l^{-1} and a pore diameter of 2 nm.

4. Analysis and discussion

The EDL effect on the concentration or on the ionic transfer at a microscopic scale appears through the K_{co} coefficients for the coions and K_{ct} for the counterions (see Eqs. (29)–(34))) with $K_{co}<1$ and $K_{ct}>1$. Thus, for a saturated porous medium in balance with an external solution, a significant difference of concentration between the pore solution and the external solution can occur in the pore below a certain size of diameter. The concentrations of coions and counterions will be respectively weaker and stronger than outside: this is the Donnan effect [29]. Much recent works deal with this effect in the field of the nanofiltration and electrodialysis [26,30,31,8] and in the field of clays [24,28,32]. In the field of cement-based materials, one can note the work of Goto and Roy [33] which note the semi-permeable behaviour of these materials with respect to the cations and the anions.

In the case of transport of ionic species through the porous media, the flux of coions and counterions will be respectively attenuated and amplified compared to the flux in the bulk solution (Eqs. (29) and (30)). This phenomenon will be all the more important, as the overlapping will be large. For an uncracked cement-based material, the penetration of aggressive ions such as chloride ions through the porous network could be affected by the overlapping of the diffuse layers: for the concentration of the pore solution given by Schmidt and Rostasy [27], we showed that overlapping becomes significant on the ion flux around a pore diameter of 10 nm which corresponding to the gel pores. For cement pastes with low porosity, Cui and Cahyadi [34] showed that the gel pores connect capillary pores (pores of higher dimension) between them. Thus in this case, to move through the capillary pore network, the ions must move through these gel pores and undergo the overlapping phenomena of the diffuse layers and their effects. Therefore, these gel pores can have an important role in the ionic transport phenomena (chlorides, sulphates,…) at the macroscopic level even their volumic fraction is very low.

5. Conclusions

The originality of this work lies in the modeling of the EDL effect on the ionic concentrations and on the flux over a pore cross-section of a given porous medium.

Examples were treated with ionic concentrations corresponding to cement-based materials. The conclusions, which can be drawn from this study, are:

- the EDL leads to the non-respect of the *local* electroneutrality. In a pore cross-section, the overlapping of the diffuse layers becomes significant when the diameter is of the same order of magnitude as a few Debye lengths;
- the mean concentrations of cations and anions over a cross-section of a pore can be very different in the case of an overlapping of the diffuse layers. The mean flux of the coions over a cross-section is strongly attenuated while that of counterions is increased;
- the size of the pore diameter and the OHP potential are determinant parameters on the overlapping phenomenon;
- for cement-based materials, the overlapping of the diffuse layers occurs in the gel pores rather than in capillary pores.

In order to investigate cases closer to cement based materials porous network, this study would be improved by considering more complex pore network and high concentration of pore solution containing different types of ions (monovalent, divalent or more…).

References

[1] L. Tang, Chloride transport in concrete — Measurement and prediction, Doctoral thesis, Dept. of Building Materials, Chalmers Universities of Technology, Sweden (1996).
[2] T. Zhang, Chloride diffusivity in concrete and its measurement from steady state migration testing, Ph.D. Thesis, Dpt of Building Materials, Norwegian University of Science and Technology, NTNU, Norway (1997).
[3] E. Samson, J. Marchand, Numerical solution of the extended Nernst–Planck model, J. Colloid Interface Sci. 215 (1999) 1–8.
[4] O. Truc, J.P. Ollivier, L.O. Nilsson, Numerical simulation of multi-species transport through saturated concrete during a migration test — MsDiff code, Cem. Concr. Res. 30 (2000) 1581–1592.
[5] A. Delagrave, J. Marchand, E. Samson, Prediction of diffusion coefficients in cement-based materials on the basis of migration experiments, Cem. Concr. Res. 26 (1996) 1831–1842.
[6] E. Samson, J. Marchand, K.A. Snyder, Calculation of ionic diffusion coefficients on the basis of migration test results, Mat. Struct. 36 (2003) 156–165.
[7] R.J. Hunter, Zeta potential in colloid science. Principles and application, Academic Press, New York, 1981.
[8] J.H. Tay, J. Liu, D.D. Sun, Effect of solution physico-chemistry on the charge property of nanofiltration membranes, Water Res. 36 (2002) 585–598.
[9] a. E. Nägele, The zeta-potential of cement, Cem. Concr. Res. 15 (1985) 453–462;
b. E. Nägele, The zeta-potential of cement Part II: effect of pH value, Cem. Concr. Res. 16 (1986) 853–863.
[10] a. E. Nägele, The zeta-potential of cement Part III: the non-equilibrium double layer on cement, Cem. Concr. Res. 17 (1987) 573–580;
b. E. Nägele, The zeta-potential of cement Part IV: effect of simple salts, Cem. Concr. Res. 17 (1987) 977–982.
[11] S. Chatterji, M. Kawamura, Electrical double layer, ion and reactions in hardened cement paste, Cem. Concr. Res. 22 (1992) 774–782.
[12] S. Chatterji, Colloid electrochemistry of saturated cement paste and some properties of cement based materials, Adv. Cem. Based Mat. Res. 22 (1998) 102–108.
[13] L. Nachbaur, P.C. Nkinamubanzi, A. Nonat, J.C. Mutin, Electrokinetic properties which control the coagulation of silicate suspension during early age hydratation, J. Colloid Interface Sci. 202 (1998) 261–268.
[14] H. Viallis-Terrisse, A. Nonat, J.C. Petit, Zeta-potential study of calcium silicates hydrates interacting with alkaline cations, J. Colloid Interface Sci. 244 (2001) 58–65.
[15] O. Amiri, A. Aït-Mokhtar, P. Dumargue, G. Touchard, Electrochemical modelling of chloride migration in cement based materials Part I: theoretical basis at microscopic scale, Electrochim. Acta 46 (2001) 1267–1275.
[16] O. Amiri, A. Aït-Mokhtar, P. Dumargue, G. Touchard, Electrochemical modelling of chloride migration in cement based materials Part II: experimental study-calculation of chlorides flux, Electrochim. Acta 46 (2001) 3589–3597.
[17] L. Antropov, Electrochimie théorique, Edition Mir, Moscou, 1979.
[18] A.J. Bard, L.R. Faulkner, Electrochimie, tome 1, Masson, Paris, 1983.
[19] John S. Newman, Electrochemical Systems, 2nd Edition Prentice Hall, Englewood Cliffs, 1991.
[20] Z. Galus, Fundamentals of electrochemical analysis, Second Edition Ellis Horwood, New York, 1994.
[21] J.P. Diard, B. Le Gorrec, C. Montella, Cinétique électrochimique, Hermann, Paris, 1996.
[22] A.W. Adamson, A.P. Gast, Physical Chemistry of surfaces, sixth edition, Wiley, New York, 1997.
[23] P.W. Atkins, Chimie physique, 6ème édition, De Boeck Université, Paris, 1999.
[24] M. Ochs, M. Boonekamp, H. Wanner, H. Sato, M. Yui, A quantitative model for ion diffusion in compacted bentonite, Radiochim. Acta 82 (1998) 437–443.
[25] H. Londiche, F. Lancelot, Les phénomènes électrocinétiques et leurs applications aux écoulements dans les milieux poreux, Ann. Mines 191 (1984) 103–108.
[26] M. Dubois, T. Zemb, L. Belloni, A. Delville, P. Levitz, R. Setton, Osmotic pressure and salt exclusion in electrostatically swollen lamellar phases, J. Chem. Phys. 96 (3) (1992) 2278–2286.
[27] F. Schmidt, F.S. Rostasy, A method for calculation of the chemical composition of the concrete pore solution, Cem. Concr. Res. 23 (1993) 1159–1168.
[28] J.F. Dufrêche, V. Marry, O. Bernard, P. Turq, Models for electrokinetic in montmorillonite, Colloids Surf., A 195 (2001) 171–180.
[29] F.G. Donnan, Theorie der Membrangleichgewichte und Membranpotentiale von nicht dialysierenden Elektrolyten. Ein Beitrag zur physikalisch-chemischen Physiologie, Z. Elektrochem. 17 (1911) 572–581 English version: Theory of membrane equilibria and membrane potentials in the presence of non-dialysing electrolytes. A contribution to physical–chemical physiology, J. Membr. Sci. 100 (1995) 45–55.
[30] A.E. James, J.D. Stillman, D.J.A. Williams, Finite element solution of the equations governing the flow of electrolyte in charged microporous membranes, Int. J. Numer. Methods Fluids 20 (1995) 1163–1178.
[31] P.Y. Pontalier, A. Ismail, M. Ghoul, Mechanisms for the selective rejection of solutes in nanofiltration membranes, Sep. Purif. Technol. 12 (2) (1997) 175–181.
[32] M. Ochs, B. Lothenbach, H. Wanner, H. Sato, M. Yui, An integrated sorption-diffusion model for the calculation of consistent distribution and diffusion coefficients in compacted Bentonite, J. Contam. Hydrol. 47 (2001) 286–296.
[33] S. Goto, D.M. Roy, Diffusion of ions through hardened cement pastes, Cem. Concr. Res. 11 (1981) 751–757.
[34] L. Cui, J.H. Cahyadi, Permeability and pore structure of OPC paste, Cem. Concr. Res. 31 (2001) 277–282.